

Breast Tumor Classification using Short-ResNet with Pixel-based Tumor Probability Map in Ultrasound Images

Ultrasonic Imaging
2023, Vol. 45(2) 74–84
© The Author(s) 2023
Article reuse guidelines:
sagepub.com/journals-permissions
DOI: 10.1177/01617346231162906
journals.sagepub.com/home/uix



You-Wei Wang¹, Tsung-Ter Kuo², Yi-Hong Chou², Yu Su²,
Shing-Hwa Huang³, and Chii-Jen Chen⁴ 

Abstract

Breast cancer is the most common form of cancer and is still the second leading cause of death for women in the world. Early detection and treatment of breast cancer can reduce mortality rates. Breast ultrasound is always used to detect and diagnose breast cancer. The accurate breast segmentation and diagnosis as benign or malignant is still a challenging task in the ultrasound image. In this paper, we proposed a classification model as short-ResNet with DC-UNet to solve the segmentation and diagnosis challenge to find the tumor and classify benign or malignant with breast ultrasonic images. The proposed model has a dice coefficient of 83% for segmentation and achieves an accuracy of 90% for classification with breast tumors. In the experiment, we have compared with segmentation task and classification result in different datasets to prove that the proposed model is more general and demonstrates better results. The deep learning model using short-ResNet to classify tumor whether benign or malignant, that combine DC-UNet of segmentation task to assist in improving the classification results.

Keywords

breast cancer, tumor classification, convolutional neural network, deep learning, ultrasound

Introduction

Breast cancer is the most common form of cancer to statistics by the International Agency for Research on Cancer (IARC, <https://www.iarc.who.int/>), and is still the second leading cause of death for women in the world.¹ However, early detection and treatment can reduce mortality rates.² Mammograph can find microcalcifications and small tumors that are the primary imaging method for early breast cancer detection.^{3,4} In addition, dense breast tissue can conceal tumors, which reduces the sensitivity of mammography.⁵ Breast ultrasound is always used to detect and diagnose breast tumors. Conventionally, 2D handheld breast ultrasound was used as an adjunct modality with the mammography which is time-consuming and operator-dependent.^{3,4} Accurate breast segmentation is still a challenging task in the ultrasound image because that have speckle noise, shadows, and ambiguous boundaries. Breast tumor segmentation can help the early diagnosis of breast cancer from handheld ultrasound images. The ultrasound image has many similar regions/pixels a similar appearance as the breast lesions.

Incorporating these regions/pixels could provide different features to learning for ultrasound breast tumor detection. The accuracy of detection is a long-standing topic in medical image processing.^{6–8} The goal is to increase the performance of breast screening using a computer-aid diagnosis (CAD) system to help radiologists to detect and diagnose breast cancer. The performance of CAD systems has some limitation because handcrafted features are operator dependent, that is

¹Department of Computer Science and Information Engineering, National Taiwan University, Taipei, Taiwan

²Department of Medical Imaging and Radiological Technology, Yuanpei University of Medical Technology, Hsinchu, Taiwan

³Department of Breast Surgery, En Chu Kong Hospital, New Taipei City, Taiwan

⁴Department of Computer Science and Information Engineering, Tamkang University, New Taipei City, Taiwan

Corresponding Author:

Chii-Jen Chen, Department of Computer Science and Information Engineering, Tamkang University, No. 151, Yingzhuang Road, Tamsui District, New Taipei City 251301, Taiwan.
Email: cjchen@mail.tku.edu.tw

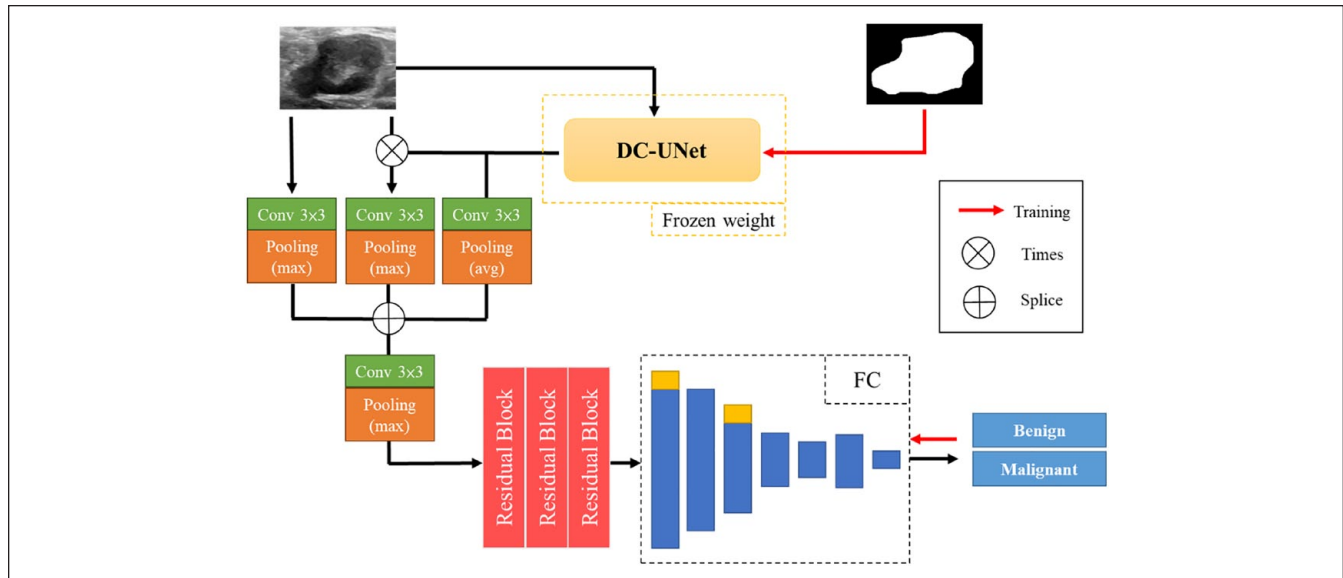


Figure 1. The processing flow of the proposed breast tumor classification network in this study. (i) We first used DC-UNet to extract the mask of the tumor. (ii) We create the model as three inputs to go through discriminate benign or malignant.

difficult to create the hand-crafted features as a challenge to describe the breast tissue.

Image segmentation is the most important task in medical image processing, that have some automatic and semi-automatic methods to extract the region of interest (ROI).^{9–11} The traditional segmentation methods have been divided into three parts: region-based method, threshold method, and clustering method. Those methods cannot suit each experimental case. In recent years, convolutional neural networks (CNN) have been the most breakthrough in the study of computer vision and digital image processing including classification, segmentation. FCN,¹² SegNet,¹³ and U-Net¹⁴ are the famous segmentation CNN model that used a network ensemble by whole convolutional layers to perform the semantic segmentation. Especially, the architecture of U-Net is symmetric, there have encoder to extract features as convolution layer and downsampling from images, and also use decoder to reconstruct segmentation results as convolution layer and upsampling, which has been the most popular architecture in medical imaging processing.¹⁴ Ibtehaz and Rahman proposed MultiResUNet found out that the original U-Net seems to be lacking in certain aspects.¹⁵

To classify benign and malignant tumors, the most direct way is to rely on radiologists to discriminate between benign and malignant tumors, but the diagnosis results due to the technology and experience of different doctors. Texture and morphological features are always used to classify benign and malignant tumors. The traditional methods are combined texture and morphological features to discriminate whether benign and malignant tumor^{16–18} is to use machine learning to train the basic model like support vector machine (SVM),¹⁹

random forest²⁰ and linear regression model. We focus on deep classification model design in this study. In recent years, the research of deep learning has changed fast, such as the earliest model called LeNet,²¹ Inception,²² and ResNet.²³

In this study, we proposed a classification model that combined the segmentation task to boost the classification accuracy and will be a pipeline to solve the challenge to find the tumor and classify benign or malignant with breast ultrasound images. We first used a segmentation network called DC-UNet²⁴ to extract the mask of breast tumors. And, we use the output of segmentation results, which are the tumor region and mask, to process with a deep learning model to discriminate whether benign or malignant tumor.

Materials and Methods

The main idea of the proposed breast tumor classification network is to combined two parts of deep learning processing that are DC-UNet as segmentation part to generate the mask of a tumor, and modified image representation layer with ResNet as classification whether the tumor is benign or malignant. As it evolves, DC-UNet is responsible for making the mask information to assist the proposed model to classify. The processing flow of the breast tumor classification network illustrates the steps as shown in Figure 1.

Image Acquisition

This study evaluates the proposed segmentation model on the two images dataset: the solid breast tumors for ultrasound images (s-BRTUS) which is our collected dataset, and the

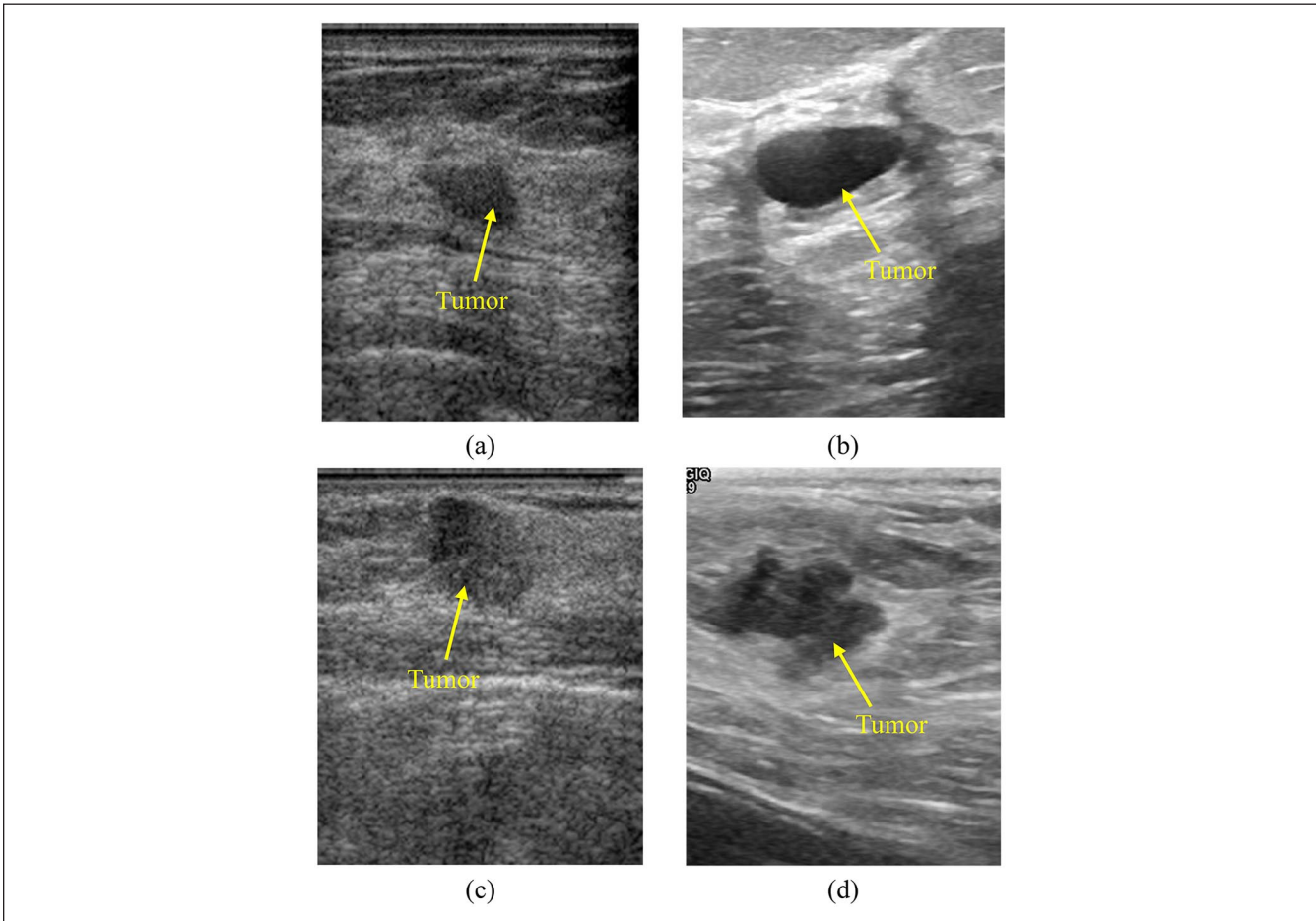


Figure 2. Tumor in breast ultrasound images. (a and b) are the benign tumor. (c and d) are the malignant tumor. (a and c) are in s-BRTUS dataset. (b and d) are in pub-BRUS dataset.

public breast ultrasound dataset (pub-BRUS).²⁵ The acquired images were transformed from DICOM to BMP format and stored as 8-bit files that ranged from 0 to 255, as shown in Figure 2(a) to (d), are from different datasets. The yellow arrow indicates the tumor in the images. The s-BRTUS comprises 806 ultrasound images of pathologically proved solid breast tumors. Real-time B-mode scanners (Voluson 530) are used with a 5 to 10 MHz transducer to extract 502 benign and 304 malignant tumors. All of the images were solid breast masses between 20 and 67 years old and supported by the authors. The mean age is 45 years old that images with an average image size of 168×226 pixels. The pub-BRUS is collected at Baheya hospital.²⁵ There are used in the scanning process are LOGIQ E9 ultrasound system and LOGIQ E9 Agile ultrasound system. The transducers are 1e5 MHz on ML6-15-D Matrix linear probe. In total, the pub-BRUS collected 780 US images with an average image size of 500×500 pixels among women ages 25 to 75 years old and 600 female patients. The images are categorized into 487 benign cases, 210 malignant, and 133 normal cases. We randomly choose 2:1:1 of ultrasound images for the training set, validation set, and test set in the experiment. Overall, the

three experiment image sets are 220, 110, and 110 benign tumors, and 128, 64, 64 malignant tumors in the s-BRTUS dataset; We also have 218, 109, and 109 benign tumors and 100, 50, 50 malignant tumors in the pub-BRUS dataset.

Image Representation

In this section, we have to decide which are inputs to the proposed model. We use the region of interest (ROI), the rectangle region, to circle the tumor on the ultrasound image. The ROI was encircled as close as possible and covered the tumor drawn by the radiologist, as shown in Figure 3. All of the images have two categories benign and malignant tumors. Therefore, the primary purpose of this paper is to classify which tumor is benign or malignant. The input ROI is resized to 320×240 . The next step of the ROI decision is to extract the feature with the ROI called image representation. The image representation has two main methods are convolution and pooling. About the convolution, we use 2D convolution to set up the model. The kernel size that we used is 3×3 , and we have chosen uniform Xavier initialization to generate the initial weight to the kernel. After convolution, we have the

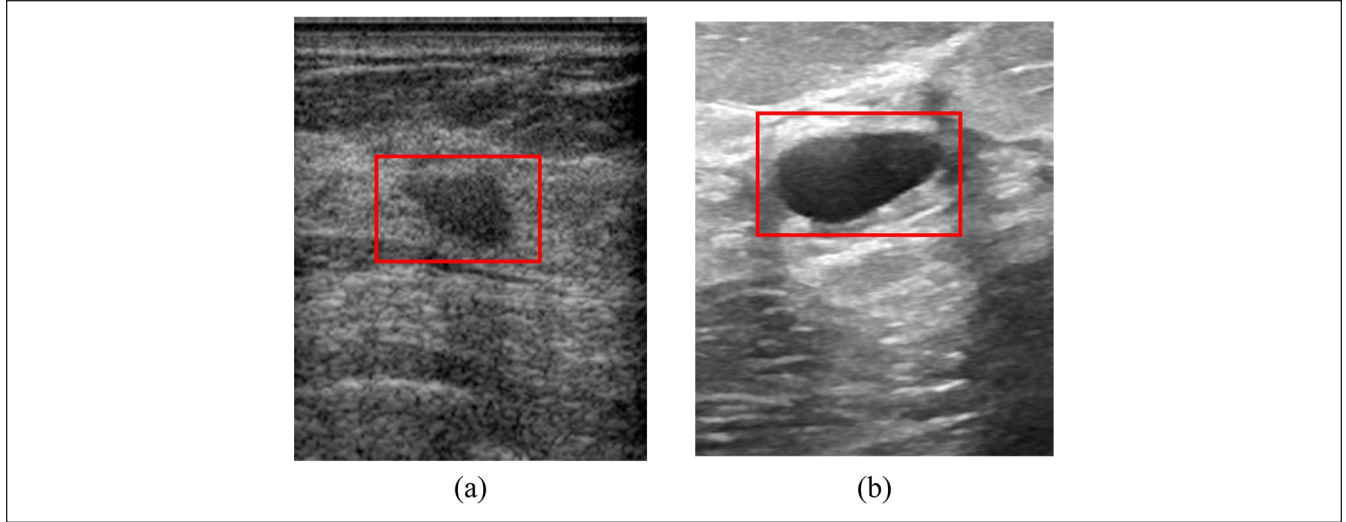


Figure 3. The ROI of tumor in different dataset. (a) is the ROI example in s-BRTUS dataset. (b) is the ROI example in pub-BRUS dataset.

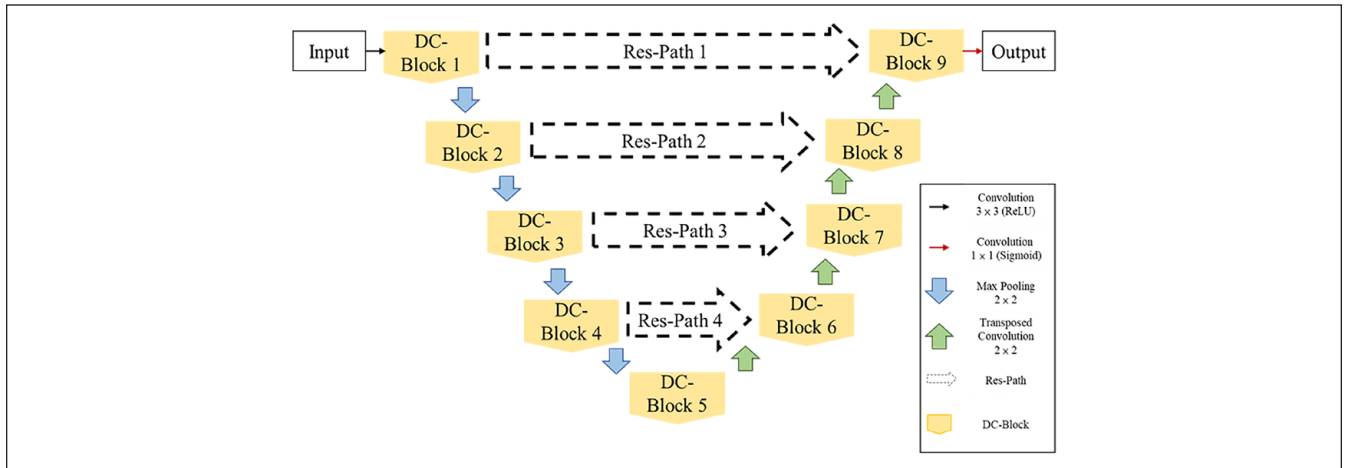


Figure 4. The processing flow of DC-UNet.

high dimension of the features as the breast tumor in the ultrasound image. All of the deep learning models to reduce the feature dimension are used pooling to ensure the diversity of different features by the convolution. Pooling has different types to generate features. There is max pooling, min pooling, and average pooling, which is chosen by what is specific to the image or the target. We used max pooling 2×2 to extract the diversity feature as a convolution in this study.

The Segmentation Task

The U-Net is the most popular segmentation model as deep learning in medical image processing.¹⁴ and that has an advanced model called the MultiResUNet.²⁴ The output of

the MultiResUNet has better segmentation results than the traditional U-Net. Because of the MultiResUNet generate more feature to the target to have effective segmentation results. In this paper, we use DC-UNet that is proposed by Lou et al.²⁴ to do the segmentation on breast US images as the parts of the proposed model. The processing flow of DC-UNet is shown in Figure 4. DC-UNet is the next-generation model of the MultiResUNet that also provides different-scale features.²⁴ Both U-Net, MultiResUNet, and DC-UNet are the pixel-based segmentation model of deep learning. Those three models can extract the probability map of the segmentation result. Here we beginning to introduce the DC-UNet. DC-UNet has two specific blocks: Res-Path and Dual-Channel block, which modified the traditional U-Net as convolution block and skip connection.²⁴ Res-Path

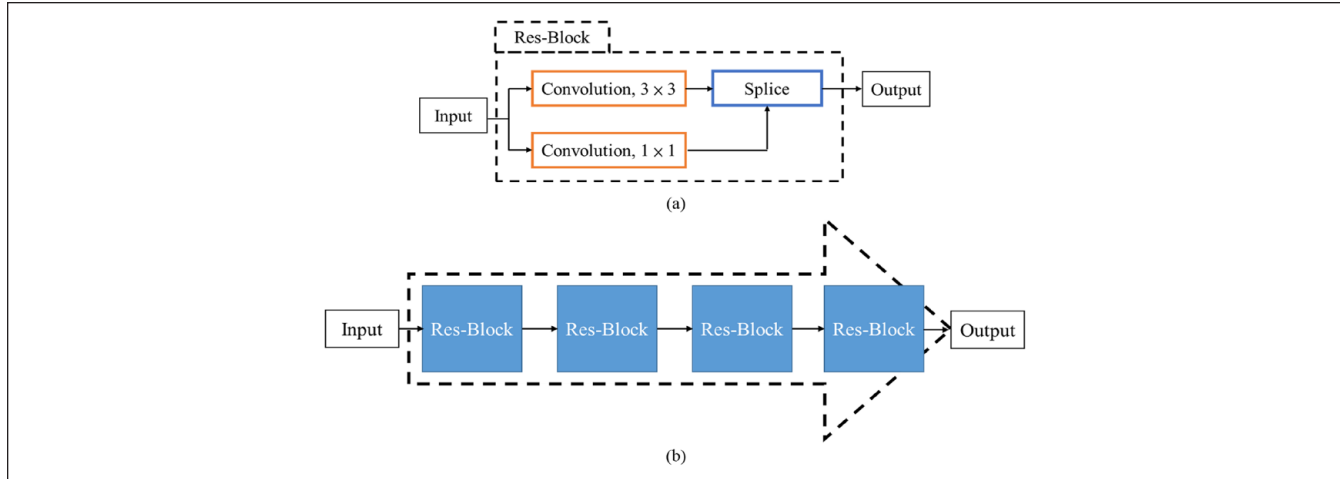


Figure 5. The detail of the Res-Path. (a) shows Res-Block. (b) is the Res-Path that used in DC-UNet.

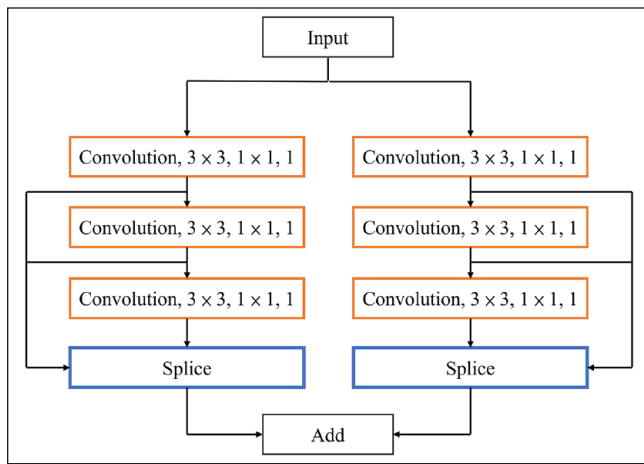


Figure 6. Dual-Channel block.

is the ResNet-like path to replace skip connection between encoder and decoder procedure, and the detail of Res-Path is shown in Figure 5. Figure 5(a) is called Res-Block to provide residual features to the next layer. The architecture of Res-Path has combined a sequence of four convolution layers with residual information in Figure 5(b), and the Dual-Channel block is shown in Figure 6. The Dual-Channel block is the inception-like block that has two same processing sequences called that Dual-Channel to have more spatial features to take a sequence of three convolution layers with the residual connection.

The Classification Model

In this section, we introduce the input of the proposed model at the beginning. We have three inputs of the classification model that are the only ROI, the mask of a tumor, and the ROI times the probability map generated by the DC-UNet as

the mask of a tumor. The mask of tumor has generated by the DC-UNet that we have the pixel-based probability map of tumor on the previous section. Next, those three inputs are going through the convolution and pooling layers to generate the features of the tumor. Then, we combine all of the features to go to the next processing stage that we use ResNet as the residual learning framework. The residual learning framework can help to preserve good results through a network with the previous layers. This has a shortcut connection to fit the input of previous layer to the next layer. Figure 7 is a sample for the residual learning framework called ResNet, that Figure 7(a) is an example for a 64-dimension basic residual block with 3×3 convolution, Figure 7(b) is a sample of ResNet pipeline, and Figure 7(c) is the ResNet pipeline we use in the proposed model. The input image can go through the modified ResNet to have feature representation. In the final step, we use seven fully connected (FC) layers to classify the feature as shown in Figure 1, blue blocks represent FC layers and yellow blocks indicate to have dropout rate as 0.9 and to have the score as tumor whether benign and malignant. The detail of the proposed model as shown in Table 1.

Experimental Results

Comparison of the Segmentation Results With Different Model

We compare the segmentation part of the proposed model with the popular segmentation deep learning models. According to provide a fair comparison, we only compare with the pub-BRUS dataset to test the mask generated part in the proposed model. In the comparison, we have FPN,¹² UNet,¹⁴ UNet+,²⁶ and DC-UNet,²⁴ all of the four deep learning models are segmentation architecture. In Table 2, we evaluate the mean values as the performance metrics

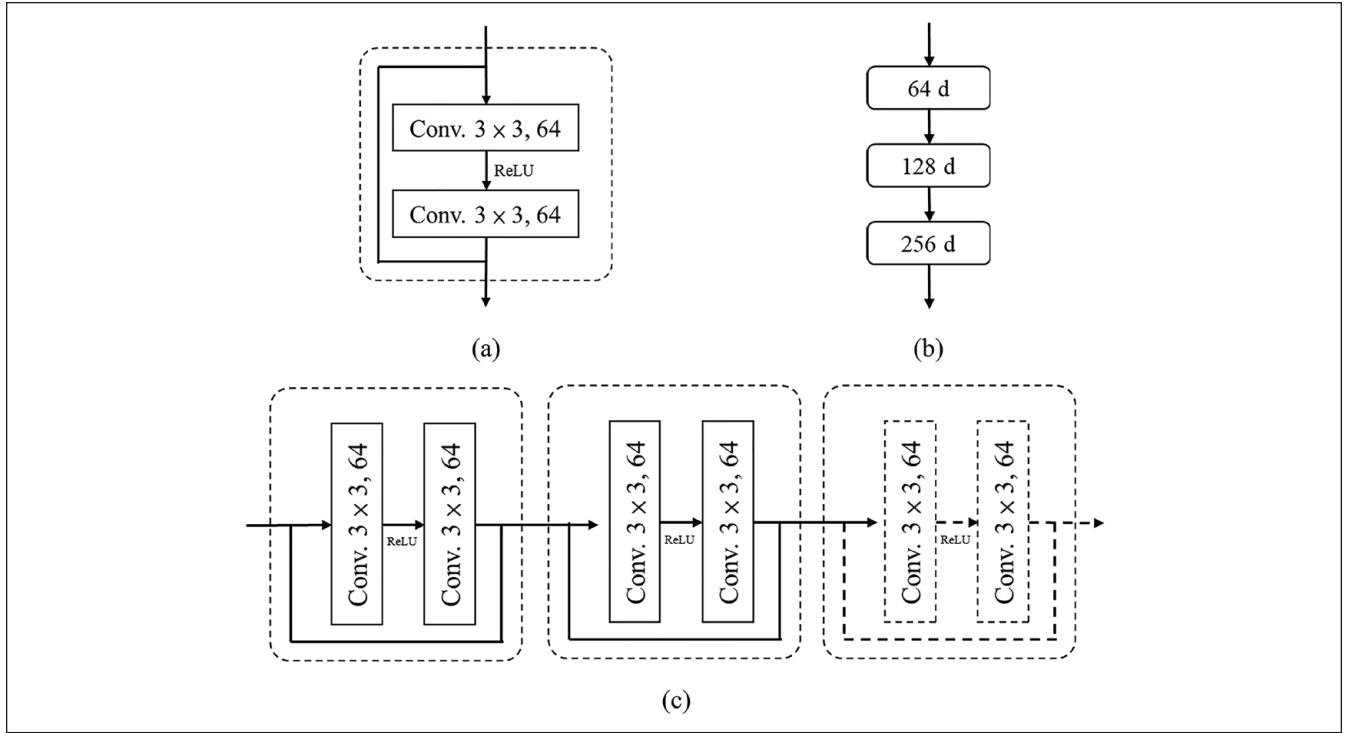


Figure 7. The detail of ResNet. (a) is 64-dimension of basic block. (b) is the example of the ResNet pipeline. (c) is the component that we used three 64-d residual blocks.

Table 1. The Detail of the Proposed Model.

	Convolution with Pooling	Residual Block	FC layer
Detail of The Proposed Model	Conv. with size 3×3 , stride 1×1 , 32 masks Max/Average Pooling with size 3×3 , stride 2×2	Conv. with size 3×3 , stride 1×1 , 64 masks Relu Conv. with size 3×3 , stride 1×1 , 64 masks After three Residual Blocks Using Max Pooling with size 4×4 , stride 2×2	FC layer 100-dim. with dropout rate: 0.8 FC layer 80-dim. FC layer 76-dim. with dropout rate: 0.8 FC layer 64-dim. FC layer 32-dim. FC layer 64-dim. Output Benign/Malignant

as intersection over union (IoU), dice, accuracy, recall, and precision on the pub-BRUS dataset. Compared with different segmentation models, DC-UNet has the better Dice score of 0.83 that shows the method is more suitable to segment the tumor of ultrasound images on the pub-BRUS dataset, because we choose DC-UNet to be a segmentation task of the proposed model. The results images are shown in Figure 8 that processed by DC-UNet.

Accuracy of the Proposed Model

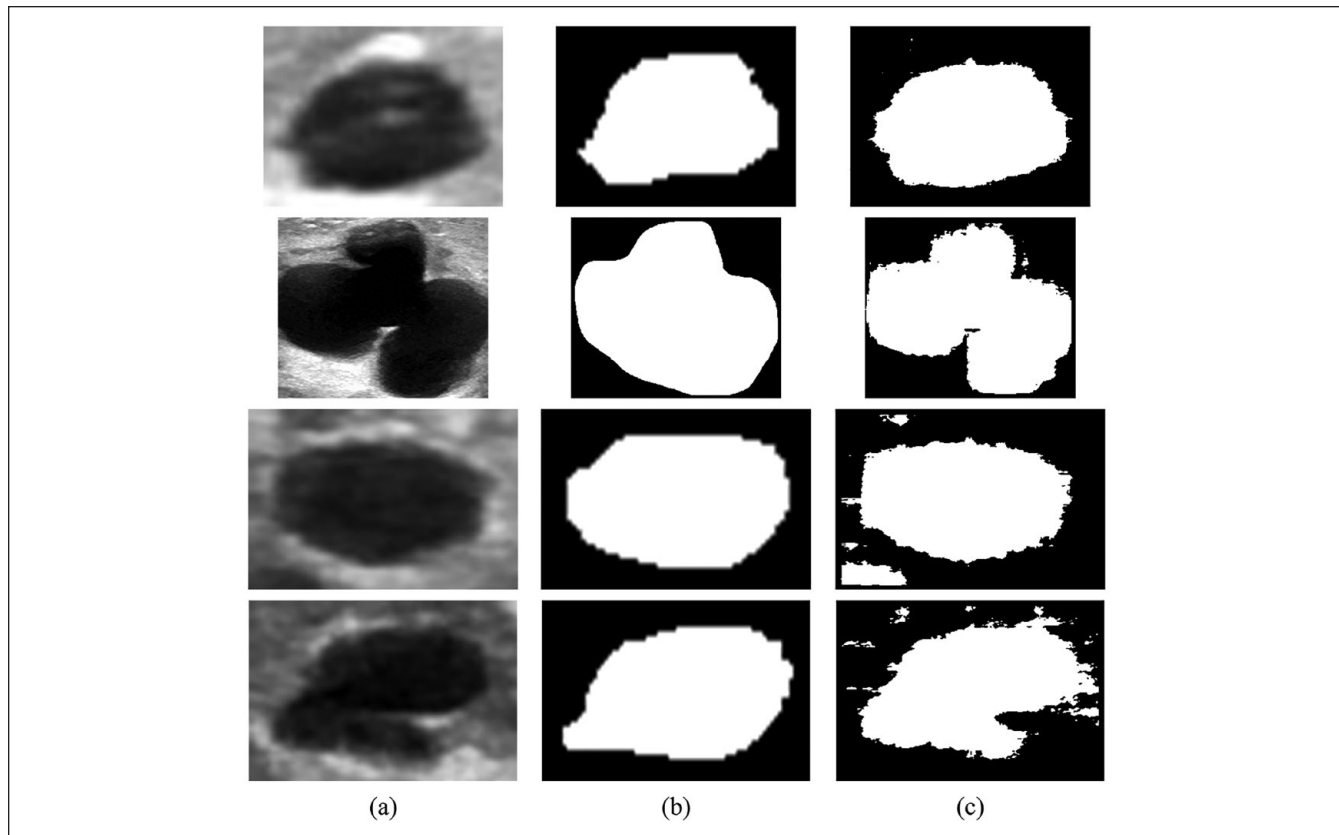
We show the results of the proposed model as tumor classification on two different datasets including the s-BRTUS and pub-BRUS dataset. The performance metrics are accuracy,

sensitivity, specificity, positive predictive value (PPV), negative predictive value (NPV), and area under the curve of ROC (AUC) used to analyze the performance on a different dataset. We train the model used two datasets, Table 3 shows results that compare the different datasets to use the proposed method. The proposed method achieves an accuracy of 97% for the s-BRTUS dataset; The proposed method achieves an accuracy of 81% for the pub-BRUS dataset. In total, the accuracy of 90% with all of the images of two datasets. In addition to the validation of different datasets to the proposed model, we used ROC curves as shown in Figure 9 for the classification results of the tumor, and we also have the value of AUC in Table 3. The model test on the s-BRTUS dataset has an AUC of 0.99 and the test on the pub-BRUS dataset

Table 2. The Comparison of Four Segmentation Models With Four Performance Metrics.

	IoU	Dice	Accuracy	Recall	Precision
FPN (12)	0.72	0.80	0.96	0.79	0.85
UNet (14)	0.64	0.73	0.96	0.70	0.83
UNet+ (26)	0.56	0.66	0.95	0.63	0.78
DC-UNet (24)	0.7	0.83	0.96	0.89	0.79

The performance results of FPN, UNet and UNet+ are provided by Xue et al.²⁷

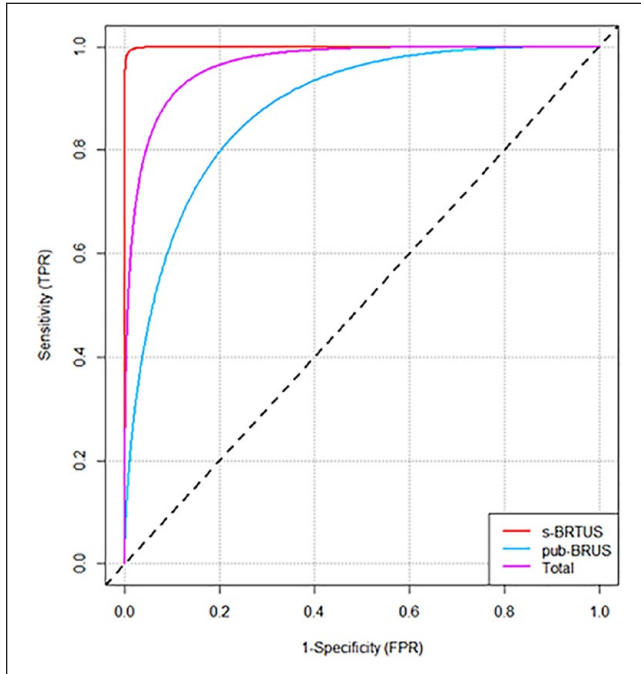
**Figure 8.** The segmentation results of DC-UNet. (a) are the targets of ultrasound image. (b) is the set of ground truth. (c) are the segmentation results.

has an AUC of 0.88. We choose the confidence intervals calculated with 200 boot samples and 90% confidence level. The best AUC is 0.99 to test the s-BRTUS dataset that is our collected data. By comparing the s-BRTUS and pub-BRUS datasets, we find out that the proposed model is more efficient to classify the s-BRTUS dataset. Table 4 shows the results of the test statistic, both DeLong's test and Venkatraman's test with 200 boots samples are significant (p -value < .05) improvement on the s-BRTUS dataset. The reason is the images have to do normalization to the same pixel spacing in the s-BRTUS dataset, the pub-BRUS dataset may not have a consistent gold standard and have the measurement notation (dash line) affect the proposed model on the images. When using the other classification method with

pub-BRUS dataset, the accuracy of AlexNet is 58%, VGG16 with transfer learning is 70%, Inception with transfer learning is 68%, ResNet with transfer learning 79%, NASNet with transfer learning is 83%.²⁸ The result shows the proposed model has a better classification of whether benign tumor and malignant tumor on the s-BRTUS dataset. Figure 10 shows the classification heatmap results in two categories, benign and malignant, which also have the ROI of original US images to take with the heatmap and presents the heatmap that visualizes the last convolution layer to know the proposed model, which is the focused region. When the proposed model discriminated ROI in the benign category, where the red area means the model with strong attention in this region that refers to the part of the inside region of the

Table 3. The Performance of the Proposed Model in Different Dataset.

		s-BRTUS		pub-BRUS		Total	
		Predicted condition		Predicted condition		Predicted condition	
		Positive (malignant)	Negative (benign)	Positive (malignant)	Negative (benign)	Positive (malignant)	Negative (benign)
Actual condition	Positive (malignant)	60	4	42	8	102	12
	Negative (benign)	2	108	18	91	20	199
Accuracy		0.97		0.84		0.9	
Sensitivity		0.94		0.84		0.89	
Specificity		0.98		0.83		0.91	
PPV		0.97		0.7		0.84	
NPV		0.96		0.92		0.94	
AUC		0.99		0.88		0.97	

**Figure 9.** ROC curves diagram: comparison of the results in different datasets.

tumor; When the proposed model discriminated ROI in the malignant category, where the closed to the red color area means the model with great attention in this region that refers to the part of the boundary of the tumor, and maybe not have strong attention in the breast tumor. The heatmap results can match the clinical experience and are interpretable and practical for the proposed model.

Comparison With the Different Task of the Proposed Model

We compare the effectiveness of the mask task with DC-UNet and without DC-UNet in the proposed model. The classification model test with or without DC-UNet as the mask task on

Table 4. The Test Statistic of the Proposed Model to Test With s-BRTUS and pub-BRUS Datasets.

	p-Value
DeLong's	1.816e-08*
Venkatraman's	<2.2e-16*

(* $p < .05$)

two datasets. Table 5 shows the seven-performance metrics are accuracy, sensitivity, specificity, PPV, NPV, and AUC used to analyze the performance on different components with DC-UNet or without DC-UNet. The proposed model with DC-UNet has an accuracy of 0.9; The proposed model without DC-UNet has an accuracy of 0.88. ROC curves diagram is shown in Figure 11, the model with DC-UNet has AUC of 0.97 and without DC-UNet has AUC of 0.95. And, Table 6 shows the results of the test statistic, both DeLong's test and Venkatraman's test with 200 boots samples are not significantly different in the proposed model with DC-UNet and without DC-UNet, but the model with DC-UNet on the performance matrix indeed improve the classification results. Therefore, the validation shows the proposed classification model with DC-UNet has better accuracy, which means that the DC-UNet segmented the mask of breast tumor in the model also contributes to the breast tumor classification performance.

Discussion

The methods introduced in this study are created the deep learning model combining the segmentation task to provide the pixel-based probability map of the tumor mask to assist the proposed model in classifying the tumor, whether benign or malignant and automated analysis on two different datasets. In the experiment, we first analyze which segmentation network is to have higher performance. The compared results show that the DC-UNet has better segmentation results, so we used that to be the segmentation task in the proposed model. There are also many great models for segmentation task that

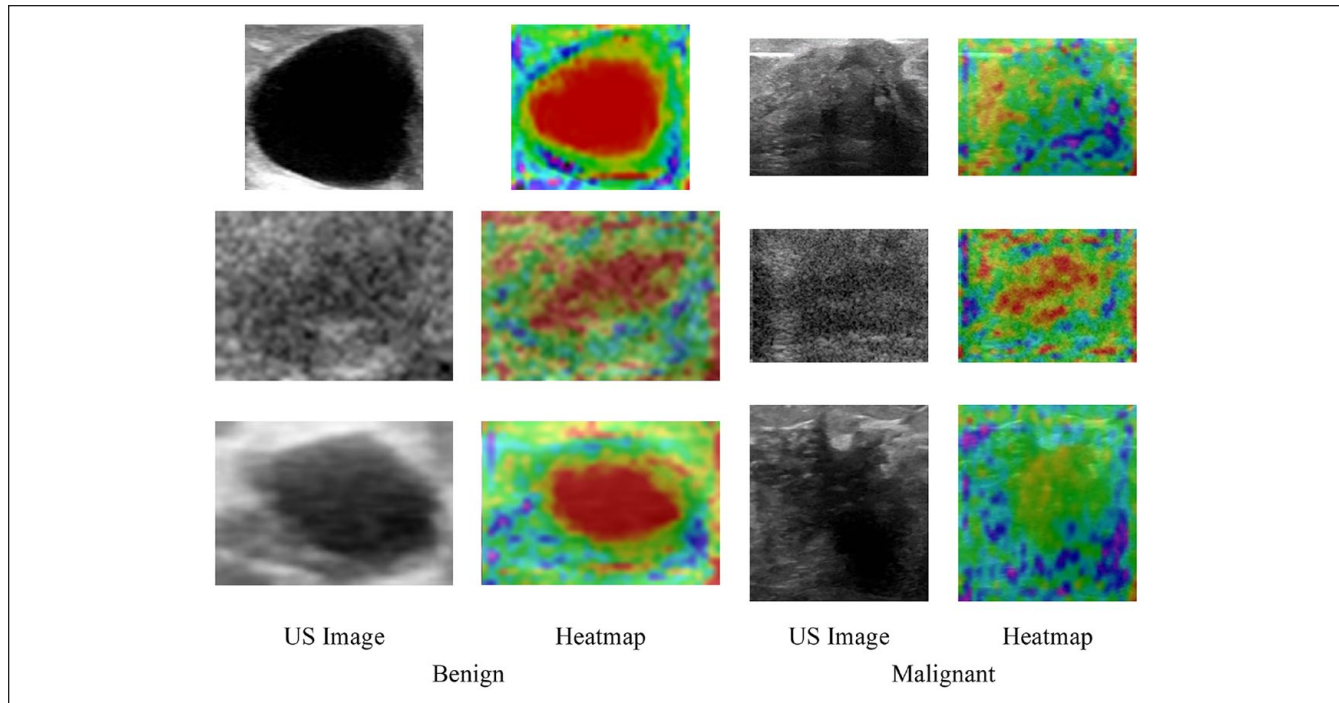


Figure 10. The classification heatmap of the last convolution in the proposed model.

Table 5. Comparison of the Proposed Model With DC-UNet and Without DC-UNet.

The proposed model	With DC-UNet		Without DC-UNet	
	Predicted condition		Predicted condition	
	Positive (malignant)	Negative (benign)	Positive (malignant)	Negative (benign)
Actual condition positive	102	12	103	11
Actual condition negative	20	199	28	191
Accuracy	0.9		0.88	
Sensitivity	0.89		0.9	
Specificity	0.91		0.87	
PPV	0.84		0.79	
NPV	0.94		0.95	
AUC	0.97		0.95	

can be used recently, such as Zhu et al.²⁹ proposed a second-order subregion pooling network for breast lesion segmentation, which can be used as a replacement option for DC-UNet. We consider that the tumor masks generated by the DC-UNet from all datasets were more correct than the four famous segmentation models. Next, we show the proposed model to train with all of the datasets. We demonstrated that the model is more suitable for the s-BRTUS dataset because the dataset has normalization with pixel spacing, is about the same size tumor, and does not have doctor notation (e.g., the

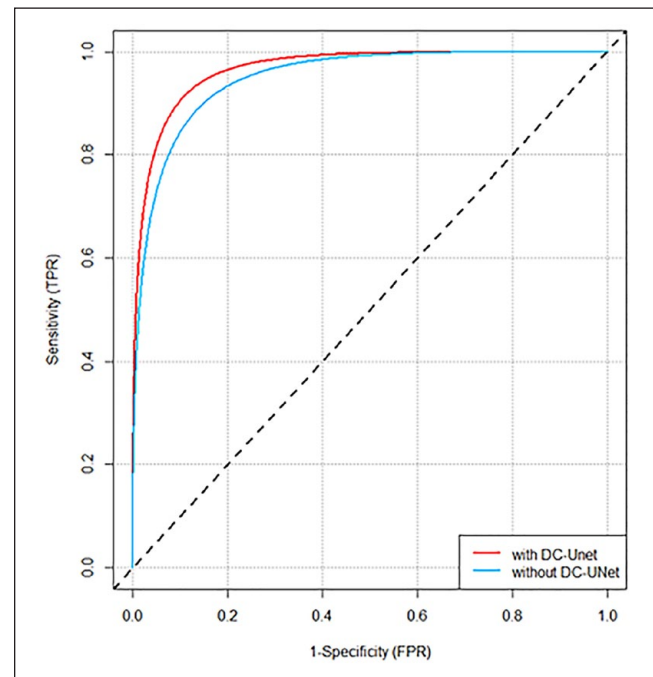


Figure 11. ROC curves diagram: comparison of the proposed model with DC-UNet and without DC-UNet.

measurement of dash line) on the images the authors prepare. In the last comparison in the experiment section, we test the segmentation component of the proposed model. The analysis results show that the model with the segmentation task as

Table 6. The Test Statistic of the Proposed Model to Test With DC-UNet and Without DC-UNet.

	p-Value
DeLong's	0.7581
Venkatraman's	0.675

(* $p < .05$)

DC-UNet has higher accuracy in classifying tumors in this study. Furthermore, the proposed model has a more suitable classification on the s-BRTUS dataset to discriminate the benign and malignant tumors.

Conclusion

This study presents an architecture to classify tumor whether benign or malignant, that combine a segmentation network called DC-UNet to assist in improving the performance of the classification model to have the mask feature as the tumor. We evaluate the proposed model on the s-BRTUS dataset and public dataset of breast tumor classification in ultrasound images. The performance achieved an accuracy of 0.9 in two datasets that can provide tumor benign/malignant information to physicians for diagnosing breast cancer. We also show the segmentation task has a higher segmentation accuracy than other famous segmentation models.

Declaration of Conflicting Interests

The author(s) declared no potential conflicts of interest with respect to the research, authorship, and/or publication of this article.

Funding

The author(s) disclosed receipt of the following financial support for the research, authorship, and/or publication of this article: This work was supported by the National Science and Technology Council of Taiwan [MOST111-2637-M-264-001].

ORCID iD

Chii-Jen Chen  <https://orcid.org/0000-0003-4280-638X>

References

1. Siegel RL, Miller KD, Jemal A. Cancer statistics, 2020. *CA Cancer J Clin.* 2020;70(1):7-30.
2. Sung H, Ferlay J, Siegel RL, Laversanne M, Soerjomataram I, Jemal A, et al. Global Cancer Statistics 2020: GLOBOCAN estimates of incidence and mortality worldwide for 36 cancers in 185 countries. *CA Cancer J Clin.* 2021;71(3):209-49.
3. Roubidoux MA, Helvie MA, Lai NE, Paramagul C. Bilateral breast cancer: early detection with mammography. *Radiology.* 1995;196(2):427-31.
4. Wilson TE, Helvie MA, August DA. Breast cancer in the elderly patient: early detection with mammography. *Radiology.* 1994;190(1):203-7. doi:10.1148/radiology.190.1.8259405
5. Berg WA. Supplemental breast cancer screening in women with dense breasts should Be offered with simultaneous collection of outcomes data. *Ann Intern Med.* 2016; 164(4):299-300. doi:10.7326/M15-2977
6. Moon WK, Shen YW, Bae MS, Huang CS, Chen JH, Chang RF. Computer-aided tumor detection based on multi-scale blob detection algorithm in automated breast ultrasound images. *IEEE Trans Med Imaging.* 2013;32(7):1191-200.
7. Tan T, Platel B, Mus R, Tabar L, Mann RM, Karssemeijer N. Computer-aided detection of cancer in automated 3-D breast ultrasound. *IEEE Trans Med Imaging.* 2013;32(9):1698-706.
8. Lo CM, Chen RT, Chang YC, Yang YW, Hung MJ, Huang CS, et al. Multi-dimensional tumor detection in automated whole breast ultrasound using topographic watershed. *IEEE Trans Med Imaging.* 2014;33(7):1503-11. doi:10.1109/tmi.2014.2315206
9. Xian M, Zhang Y, Cheng HD. Fully automatic segmentation of breast ultrasound images based on breast characteristics in space and frequency domains. *Pattern Recognit.* 2015;48(2):485-97.
10. Shan J, Cheng HD, Wang Y. Completely automated segmentation approach for breast ultrasound images using multiple-domain features. *Ultrasound Med Biol.* 2012;38(2):262-75.
11. Ashton EA, Parker KJ. Multiple resolution Bayesian segmentation of ultrasound images. *Ultrason Imaging.* 1995;17(4):291-304.
12. Long J, Shelhamer E, Darrell T. Fully Convolutional Networks for Semantic Segmentation. *CVPR; Boston.* 2015. pp.3431-40.
13. Badrinarayanan V, Kendall A, Cipolla R. SegNet: A deep convolutional encoder-decoder architecture for image segmentation. *IEEE Trans Pattern Anal Mach Intell.* 2017;39(12):2481-95.
14. Ronneberger O, Fischer P, Brox T. U-Net: Convolutional Networks for Biomedical Image Segmentation. *Cham: Springer International Publishing;* 2015. pp.234-41.
15. Ibtihaz N, Rahman MS. MultiResUNet : Rethinking the U-net architecture for multimodal biomedical image segmentation. *Neural Netw.* 2020;121:74-87.
16. Jebamony J, Jacob D. Classification of benign and malignant breast masses on mammograms for large datasets using core vector machines. *Curr Med Imaging.* 2020;16(6):703-10.
17. Chang R-F, Wu WJ, Moon WK, Chou Y-H, Chen D-R. Support vector machines for diagnosis of breast tumors on US images. *Acad Radiol.* 2003;10(2):189-97.
18. Ray R, Abdullah AA, Mallick DK, Ranjan Dash S. Classification of benign and malignant breast cancer using supervised machine learning algorithms based on image and numeric datasets. *J Phys Conf Ser.* 2019;1372:012062.
19. Hearst MA, Dumais ST, Osuna E, Platt J, Scholkopf B. Support vector machines. *IEEE Intell Syst Appl.* 1998;13(4):18-28.
20. Breiman L. Random forests. *Mach Learn.* 2001;45(1):5-32.
21. Lecun Y, Bottou L, Bengio Y, Haffner P. Gradient-based learning applied to document recognition. *Proc IEEE.* 1998;86(11):2278-324.
22. Szegedy C, Ioffe S, Vanhoucke V, Alemi A. Inception-v4, Inception-ResNet and the impact of residual connections on learning. In: *Proceedings of the AAAI conference on artificial intelligence*, San Francisco, 2017. doi: 10.1609/aaai.v31i1.11231.
23. He K, Zhang X, Ren S and Sun J (eds). Deep residual learning for image recognition. In: *Proceedings of the IEEE conference on computer vision and pattern recognition;* 2016.

24. Lou A, Guan S, Loew M. DC-UNet: Rethinking the U-Net Architecture With Dual Channel Efficient CNN for Medical Image Segmentation. In *Medical Imaging 2021: Image Processing*, SPIE; 2021; 11596:758-68. doi: 10.1117/12.2582338.
25. Al-Dhabyani W, Gomaa M, Khaled H, Fahmy A. Dataset of breast ultrasound images. *Data Brief*. 2020;28:104863.
26. Zhou Z, Rahman Siddiquee MM, Tajbakhsh N, Liang J. UNet++: A Nested U-Net Architecture for Medical Image Segmentation: 4th International Workshop, DLMIA 2018, and 8th International Workshop, ML-CDS 2018, Held in Conjunction with MICCAI 2018, Granada, Spain, September 20, 2018, Proceedings; 2018;11045:3-11. doi: 10.1007/978-3-030-00889-5_1.
27. Xue C, Zhu L, Fu H, Hu X, Li X, Zhang H, et al. Global guidance network for breast lesion segmentation in ultrasound images. *Med Image Anal*. 2021;70:101989. doi:10.1016/j.media.2021.101989
28. Al-Dhabyani W, Gomaa M, Khaled H, Fahmy A. Deep learning approaches for data augmentation and classification of breast masses using ultrasound images. *Int J Adv Comput Sci Appl*. 2019;10(5):1-11.
29. Zhu L, Chen R, Fu H, Xie C, Wang L, Wan L, et al. (eds) A second-order subregion pooling network for breast lesion segmentation in ultrasound. In: *International Conference on Medical Image Computing and Computer-Assisted Intervention*. Springer; 2020.